



Cite this: *Chem. Commun.*, 2025, **61**, 17244

## Supramolecular chemistry-based materials on SO<sub>2</sub> capture: recent advances

Antonio Hernández-Monsalvo,<sup>a</sup> Pablo Marín-Rosas,<sup>b</sup> Víctor M. Trejos,<sup>b</sup> Nancy E. Dávila-Guzmán,<sup>c</sup> Jose Antonio de los Reyes,<sup>d</sup> Diego Solis-Ibarra,<sup>c</sup> Enrique Lima,<sup>b</sup> Ricardo A. Peralta<sup>b</sup> and Illich A. Ibarra<sup>c</sup>

The urgent need for efficient methods to detect, monitor, and capture toxic and hazardous sulfur dioxide (SO<sub>2</sub>) has driven the development of new devices for this purpose. Due to its significant corrosiveness and high toxicity, a key requirement for adsorbent materials is their ability to withstand deterioration, alongside possessing high gas sensitivity and selectivity. Within this domain, supramolecular chemistry has made substantial inroads through the development of innovative porous materials formed by the self-assembly of molecular building blocks, driven by diverse interactions. The complex architectures that result can be categorised as either extended networks, such as metal–organic frameworks (MOFs) and covalent organic frameworks (COFs), or as molecular cages, including metal–organic cages (MOCs) and porous organic cages (POCs). These materials have demonstrated high capture capacities, extremely sensitive detection limits, and even active sites for the catalytic transformation of adsorbed molecules. This review aims to highlight the primary contributions of these supramolecular materials to the experimental adsorption of SO<sub>2</sub>, along with their most remarkable results.

Received 3rd August 2025,  
Accepted 23rd September 2025

DOI: 10.1039/d5cc04442a

[rsc.li/chemcomm](http://rsc.li/chemcomm)

<sup>a</sup> Laboratorio de Físicoquímica y Reactividad de Superficies (LaFReS), Instituto de Investigaciones en Materiales, Universidad Nacional Autónoma de México, Circuito Exterior s/n, CU, Del Coyoacán, 04510, CDMX, Mexico.

E-mail: argel@unam.mx

<sup>b</sup> Departamento de Química, División de Ciencias Básicas e Ingeniería, Universidad Autónoma Metropolitana (UAM-I), 09340, CDMX, Mexico

<sup>c</sup> Universidad Autónoma de Nuevo León, UANL, Facultad de Ciencias Químicas, Av. Universidad, Cd. Universitaria, 66455, San Nicolás de los Garza, Nuevo León, Mexico

<sup>d</sup> Departamento de Ingeniería de Procesos e Hidráulica, División de Ciencias Básicas e Ingeniería, Universidad Autónoma Metropolitana-Iztapalapa, 09340, Ciudad de México, Mexico



From left to right: Ricardo Peralta, Pablo Marín-Rosas, Antonio Hernández-Monsalvo, Enrique Lima and Illich Ibarra

## Introduction

Today, we are constantly exposed to a vast array of air pollutants. Among these, some pose a particularly significant risk, not only to human health but also to the delicate balance of ecosystems and the natural cycles of the environment. Such is the case of sulphur dioxide (SO<sub>2</sub>), a corrosive and colourless gas that the World Health Organization (WHO) classifies as one of the most toxic chemicals for humans.<sup>1</sup> What makes this gas particularly alarming is not just its rapid spread, owing to its high solubility, or its devastating effects on aquifers and plant life through acid

*Ricardo Peralta is a Full Professor at UAM who is interested in novel catalytic applications of semi-open metal sites within MOFs.*

*Pablo Marín-Rosas is a PhD Student who is exploring MOF materials for catalytic applications.*

*Antonio Hernández-Monsalvo works on his Master's degree, investigating chemically stable MOFs for the sensing of toxic chemicals. Enrique Lima serves as the Vice-Principal of the Institute for Materials Research at UNAM, and his research focuses on bio-applications of MOF materials.*

*Illich Ibarra is a Full Professor at UNAM, working on the use of MOFs for the capture and detection of toxic gases such as SO<sub>2</sub> and H<sub>2</sub>S.*



## Highlight

rain and the disruption of the natural sulphur cycle.<sup>2</sup> For example, a brief exposure to trace concentrations of this chemical – a mere 1.5 parts per million (ppm) for as little as 10 minutes – can instantly cause breathing difficulties in a healthy individual.<sup>3</sup>

In fact, air quality guidelines stipulate that the maximum tolerable human exposure to  $\text{SO}_2$  is 175 parts per billion (ppb), which equates to  $500 \mu\text{g m}^{-3}$ , for ten-minute intervals, and a daily average of  $20 \mu\text{g m}^{-3}$  (8 ppb).<sup>4</sup> Exceeding these limits can lead to serious health issues, including chronic inflammation or obstruction in the respiratory system and respiratory tract infections.<sup>5</sup> Even a few minutes of exposure to 100 ppm can be fatal due to the rapid absorption of  $\text{SO}_2$  through the skin and respiratory tract.<sup>1,6</sup> Furthermore,  $\text{SO}_2$  acts as a precursor to secondary pollutants, such as fine particulate matter (PM2.5), which are also globally recognized as highly detrimental to health.<sup>7</sup> The fact that such minute concentrations can be so harmful underscores the urgent need for highly efficient and sensitive methods to detect, monitor, and potentially capture  $\text{SO}_2$  in environments that are at risk of contamination.

In recent years, sophisticated porous materials like metal-organic frameworks (MOFs) and molecular cages (MCs) have demonstrated the ability to achieve this crucial and precise detection.<sup>8</sup> It has been previously demonstrated that these materials exhibit excellent performance in both  $\text{SO}_2$  capture and detection, not only maximizing gas uptake and storage, but also enabling cyclic reuse without compromising the inherent properties that make them such effective and sensitive adsorbents.

MOFs represent one class of porous crystalline materials based on supramolecular chemistry; they are characterized by the self-assembly of metal ions with organic ligands *via* coordination interactions,<sup>9</sup> whereas a covalent bonded assembly of light elements as building blocks (e.g., C, H, O, N, and B) leads to the formation of covalent organic frameworks (COFs)<sup>10</sup>. Similarly, supramolecular porous materials, such as molecular cages, can be generated by an analogous process. Molecular cages have internal cavities suitable for molecular storage, employing a host–guest system, and can also be differentiated by the nature of their constituent bonds. When coordination interactions are involved, it leads to metal–organic cages (MOCs),<sup>11</sup> and porous organic cages (POCs) are obtained through the self-assembly of organic monomers linked by covalent bonds.<sup>12</sup>

The reasons why MOFs, COFs, MOCs, and POCs are highly promising candidates for corrosive gas capture and sensing applications lie in the chemistry behind their formation, which is rooted in supramolecular chemistry. One of the fundamental principles of supramolecular chemistry is spontaneous self-assembly, which refers to the ability of molecules to selectively couple, as building blocks, to facilitate the formation of more complex and well-organized structures through forces considerably weaker than covalent bonds (e.g., electrostatic forces,  $\pi$ – $\pi$  interactions, hydrogen bonds and van der Waals forces).<sup>9,13</sup> The structure they adopt is derived from their self-assembly, which is responsible for their high porosity, providing both high adsorption capacity and a relatively high surface area.

Moreover, the specific types of interactions that maintain the structure of these complex materials lead to the formation of

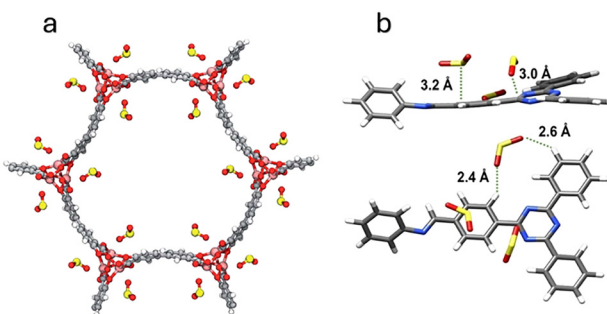


Fig. 1 Molecular recognition interaction between active sites of (a)  $\text{MOF2}^0$  and (b)  $\text{COF1}^0$  building blocks with  $\text{SO}_2$  molecules.

active sites, which function on a lock-and-key principle. When the interaction with the guest molecule (*i.e.*,  $\text{SO}_2$ ) is favourable, the active site (host) will facilitate its binding through non-covalent forces.<sup>13</sup> This exemplifies another fundamental principle of supramolecular chemistry: molecular recognition (Fig. 1). Thus, the combination of high porosity and molecular recognition provides these materials with significant advantages compared to other adsorbents.

Porous complex materials exhibit pronounced sensitivity, enhanced by guest–guest packing interactions that facilitate a more ordered arrangement of  $\text{SO}_2$  within the pores,<sup>8</sup> enabling the detection of trace amounts of  $\text{SO}_2$ . Some of these materials even possess robust structural and chemical stability, which supports facile regeneration for cyclical use without loss of crystallinity or porosity (material degradation).<sup>10–12</sup> In addition, the uptake of  $\text{SO}_2$  in the internal cavities of these materials can trigger measurable changes in their optical, electrical, or mechanical properties. This effect can be applied in the development of molecular sensors, employing techniques such as spectroscopy or electrical conductivity measurements.<sup>10</sup>

Thus, the objective of this work is to discuss the latest contributions to the meticulous design and application of these supramolecular porous materials in  $\text{SO}_2$  capture and detection. Furthermore, it aims to encourage other research groups to continue exploring the frontiers of this field, pushing the boundaries of what this branch of chemistry and materials science can achieve in terms of even greater performance.

## Advances in chemistry-based materials

The binding of  $\text{SO}_2$  to various materials of interest exhibits specific characteristics for each. The interactions governing the adsorption of  $\text{SO}_2$  molecules onto the surface are contingent upon the chemical and electronic properties of the surface. The active sites responsible for  $\text{SO}_2$  binding on the material's surface are characterised by inherent unsaturation of the binding forces between the constituent atoms of the solid structure.<sup>14</sup> Characteristic features such as pores, surface defects, and even specific functional groups serve as localities where external molecules, such as  $\text{SO}_2$ , can readily adsorb through tailored interactions favoured by the intrinsic properties of these sites.



The two oxygen atoms within the  $\text{SO}_2$  molecule predominantly act as Lewis bases, exhibiting non-bonding electrons that are readily available for donation.<sup>15</sup> Depending on the specific adsorbent material, these oxygen atoms can serve as the primary binding sites for the molecule. Their versatility allows them to engage in a spectrum of interactions, ranging from strong coordination with highly charged, poorly polarizable, low-molecular-mass metal ions (hard metals) to both strong and weak hydrogen bonds with a variety of functional groups.<sup>16</sup>

In contrast, the sulphur atom behaves as a Lewis acid, which consequently shows good affinity for accepting external electrons, making it particularly good at generating coordination bonds with electron-rich transition metals and weak S–O interactions. Similarly, if the material is porous and free of metal ions, van der Waals forces, weak noncovalent, and even covalent bonds can occur in the cavities.<sup>16,17</sup> However, these interactions are not mutually exclusive; rather, combinations of different host–guest interactions can coexist within the same material.

The quantity and spatial arrangement of active sites across the solid's surface are intricately linked to the material's electronic and geometric structure. These sites can exhibit preferential affinity for certain molecules over others, thereby imparting specificity and rendering the adsorption process selective. Consequently, this leads to a preferential order in the bonds formed between  $\text{SO}_2$  molecules and the binding sites of porous supramolecular materials.

### $\text{SO}_2$ -MOFs

Given the highly corrosive and reactive nature of  $\text{SO}_2$ , the adsorbents employed for desulfurization must demonstrate exceptional stability and reversibility. Metal–organic frameworks (MOFs) are no exception to this requirement. The strong coordination that can form between the sulphur atom of  $\text{SO}_2$  and the metallic nodes within the MOF structure can, in fact, surpass the strength of the metal–ligand bonds. Consequently, this can lead to irreversible adsorption and even boost the material's degradation.<sup>16</sup> Such deterioration may manifest as a loss of crystallinity or a reduction in surface area stemming from the permanent occupation of active sites.<sup>17,19</sup>

Indeed, adsorption reversibility and the prevention of material deterioration are just as critical as gas capture capacity and have posed significant challenges in optimizing the performance of MOFs for  $\text{SO}_2$  adsorption, particularly for applications requiring cyclic operation.

The pursuit of  $\text{SO}_2$ -adsorbing MOFs exhibiting robust stability without compromising high uptake capacities was initially spurred by MOF-177.<sup>17</sup> This material demonstrates an uptake of  $25.7 \text{ mmol g}^{-1}$  (at 293 K and 1 bar) but undergoes significant deterioration following  $\text{SO}_2$  adsorption. Subsequently, materials like UR3-MIL-101(Cr)<sup>18</sup> and MFM-422<sup>19</sup> also encountered this challenge. While achieving even higher uptakes of 36.7 and  $31.3 \text{ mmol g}^{-1}$  (at 293 K and 1 bar), they also suffered from chemical instability, surface degradation, or pore blockage, leading to reduction in porosity after the initial adsorption cycles (Fig. 2).

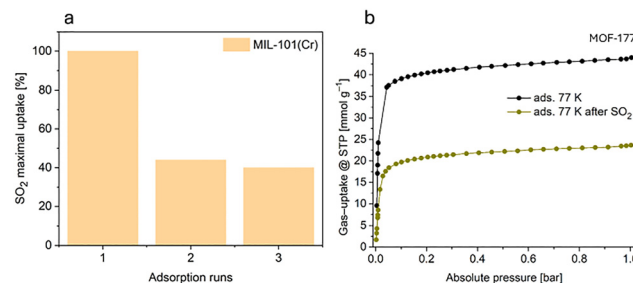


Fig. 2 Loss in gas maximum uptake for MOFs: (a) MIL-101(Cr)<sup>18</sup> and (b) MOF-177<sup>17</sup> after  $\text{SO}_2$  exposure.

More recently, significant contributions to this research have been presented with MOFs MIL-101(Cr)-4F(1%)<sup>8</sup> and  $\text{Mg}_2(\text{dobpdc})$ .<sup>20</sup>

These materials share key attributes, including noteworthy  $\text{SO}_2$  capture capacities of  $18.4 \text{ mmol g}^{-1}$  and  $19.5 \text{ mmol g}^{-1}$ , respectively (at 293 K and 1 bar) and remarkable resilience, by retaining their structural integrity, crystallinity, and surface area after  $\text{SO}_2$  adsorption under both dry and humid conditions, even after 50 cycles (Fig. 3). This underscores complete reversibility in the adsorption process, along with selective adsorption of  $\text{SO}_2$  over other gases such as  $\text{CO}_2$  or  $\text{N}_2$ .

Additionally, both MIL-101(Cr)-4F(1%) and  $\text{Mg}_2(\text{dobpdc})$  exhibit sensitive detection limits at low pressures, positioning them as promising candidates for the development of detectors and separators for gas mixtures containing  $\text{SO}_2$ .

Following this important contribution, further advancements have continued to enhance the performance of  $\text{SO}_2$ -adsorbing MOFs. State-of-the-art materials, such as the highly porous MOF Zr-TPA<sup>21</sup> and the MOF designated SJTU-220,<sup>22</sup> have achieved impressive sorption capacities of  $22.7 \text{ mmol g}^{-1}$  and  $29.6 \text{ mmol g}^{-1}$  (at 298 K and 1 bar), respectively, both exhibiting

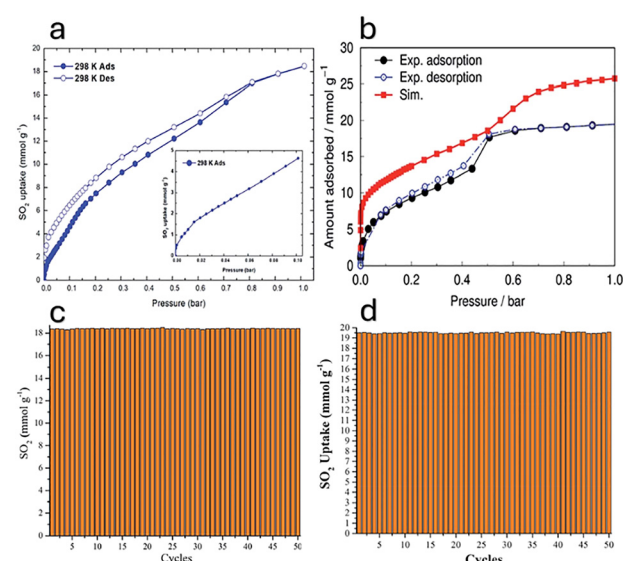


Fig. 3  $\text{SO}_2$  experimental adsorption–desorption isotherms and cycles for: (a) and (c) MIL-101(Cr)-4F(1%)<sup>8</sup> and (b) and (d)  $\text{Mg}_2(\text{dobpdc})$ <sup>20</sup> at 298 K and up to 1 bar.



## Highlight

excellent recyclability and sustained stability. Ongoing research in this application of MOFs is significantly contributing to the development and refinement of efficient  $\text{SO}_2$  adsorbent solids, while continuous progress takes us deeper into our understanding of the molecular interactions governing  $\text{SO}_2$  sorption on these supramolecular materials.

**SO<sub>2</sub>-COFs**

Similar to MOFs, covalent organic frameworks (COFs) are highly porous materials characterised by extended crystalline structures formed by exclusively linking organic molecular building blocks *via* robust covalent bonds. These inherent bonds endow COFs with exceptional stability, rendering their crystalline structure remarkably resistant to modification, even upon interaction with external agents or under harsh conditions. Consequently, they are inherently appealing for versatile adsorption and storage applications involving hazardous gases, including corrosive ones like  $\text{SO}_2$ , which contribute to atmospheric pollution.<sup>23</sup>

The inherent nature of the cross-linked functional groups within COF structures provides a diverse array of host–guest binding sites for  $\text{SO}_2$  molecules. These interactions are not limited to a single type; rather, they concurrently promote a wide spectrum of bonds with different binding strengths. While the  $\pi$ -electron densities present within the building blocks (*i.e.*, aromatic rings and nitrogen atoms' lone pairs) strongly interact with adsorbed  $\text{SO}_2$ , potentially leading to hysteresis, weaker bonds like hydrogen bonds exert a nearly imperceptible individual effect. However, collectively, these interactions facilitate both in-plane and out-of-plane adsorption along the structure of the mesoporous material.<sup>10,23</sup>

Despite these favourable attributes, the exploration of COFs as  $\text{SO}_2$  adsorbents has been relatively limited. PI-COF-m10 stands out as an early example in this area; this imine-based COF was functionalized with DMMA as a modulator to lower the energy barrier for  $\text{SO}_2$  desorption. While complete reversibility was achieved over 5 cycles with an adsorption capacity of  $6.30 \text{ mmol SO}_2 \text{ g}^{-1}$ , the incorporation of the modulator resulted in alterations to the crystal structure, leading to an increase in amorphous regions and a reduction in the overall sorption capacity.<sup>23,24</sup>

The integration of active groups or metallic atoms to dope the structure of COFs has also been proposed to improve the efficiency of these materials in capturing specific molecules such as  $\text{SO}_2$ . In COF-DC-8, the nickel atoms found throughout its 2D structure improve its three-dimensional electronic conductivity, compared to a pure organic solid. This increases the potential to amplify the alignment of  $\pi$ -conjugated units and improves charge transport through space, achieving increased sensitivity and being able to quantify gas molecules adsorbed on its surface within the order of ppb through changes in chemoresistivity.<sup>23,25</sup>

In the case of COF-105, density functional theory (DFT) calculations indicate that incorporating a single transition metal atom, Sc(III), within its building blocks can significantly promote the formation of adsorption complexes between the adsorbed  $\text{SO}_2$  gas molecule and the metal-doped COF. This

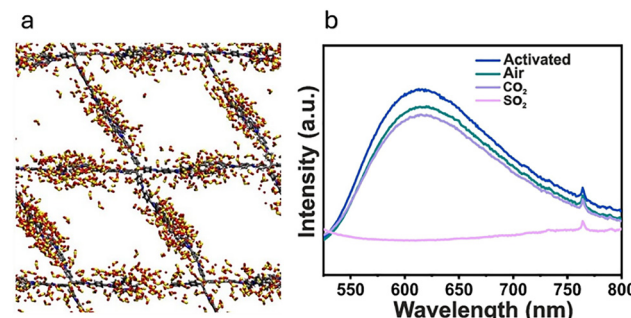


Fig. 4 SonoCOF-9: (a) structural interaction with  $\text{SO}_2$  molecules, (b) photoluminescence emission spectrum with air,  $\text{CO}_2$ , and after  $\text{SO}_2$ .<sup>10</sup>

doping strategy is predicted to enhance the interaction energy by up to an order of magnitude compared to the undoped material. This enhancement is attributed to donor–acceptor delocalization occurring between a lone pair of electrons on an oxygen atom of  $\text{SO}_2$  and the Sc(III) atom within the COF framework.<sup>23,26</sup>

Against this scenery, the most recent significant advancement in this field has been the development of SonoCOF-9.<sup>10</sup> Functionalized with imine and aromatic units, this material demonstrates remarkable chemical stability in the presence of  $\text{SO}_2$ , maintaining a consistent capture capacity of  $3.5 \text{ mmol g}^{-1}$  over 50 adsorption–desorption cycles without any loss in crystallinity or porosity. Moreover, its strong interaction energy with  $\text{SO}_2$  renders it highly selective and sensitive to this gas, capable of detecting concentrations as low as 6.4 ppb, when THF is used as a dispersing medium.

Additionally, fluorescence spectroscopy can be used to make SonoCOF-9 perform as a sensitive  $\text{SO}_2$  sensor. When  $\text{SO}_2$  molecules adsorb onto its surface, the intensity of its emission spectrum dramatically decreases (Fig. 4). This contribution underscores the considerable potential of this material for detection, without the need for doping, while also exhibiting notable selectivity for the recognition and separation of gas mixtures, since the emission lessening described does not occur with other adsorbates.

Research into the application of COFs for the adsorption of corrosive gases such as  $\text{SO}_2$  is anticipated to undergo continued expansion and intensification, to achieve optimal performance for these materials in the years ahead. The ongoing exploration of the potential in this class of materials is poised to unlock novel applications and insights that currently remain undiscovered.

**SO<sub>2</sub>-MOCs**

Metal–organic cages (MOCs) are also supramolecular structures formed through the self-assembly of metal ions and organic ligands through coordination interactions. This process yields highly symmetrical, nanometric structures featuring pseudo-spherical cavities that are ideal for encapsulating spherical guest molecules.<sup>27</sup> Moreover, MOCs demonstrate high solubility in polar solvents, including water.<sup>28</sup> Consequently, these properties make MOCs excellent candidates for molecular capture and separation applications.

Reports continuously emerge showcasing the enhanced and selective adsorption of gaseous compounds by these materials, whether in the gas phase, in solution, or even when dispersed within polymer membranes.<sup>29</sup> Beyond adsorption, their potential for heterogeneous catalysis is also being actively investigated. For instance, recent research highlights the successful application of MOCs in efficiently and selectively catalysing the conversion of chemical species such as iodine and carbon dioxide ( $\text{CO}_2$ ) on their surfaces.<sup>27,30</sup> However, the capture of  $\text{SO}_2$  using MOCs has remained largely unexplored to date.

The initial study exploring the interaction of  $\text{SO}_2$  with MOCs was published in 2021.<sup>28</sup> A palladium-based MOC, specifically  $[\text{Pd}_6\text{L}_8](\text{NO}_3)_{36}$  (referred to as cage 1) was selected for this investigation due to its well-defined hexapalladium(II) matrix. This material, exhibiting a pseudo-cubic molecular structure, demonstrated a remarkable  $\text{SO}_2$  adsorption capacity of  $6.0 \text{ mmol g}^{-1}$  at 1.0 bar, especially considering its relatively modest surface area of  $111 \text{ m}^2 \text{ g}^{-1}$ . This significant finding underscored the effectiveness of cage 1 for competent  $\text{SO}_2$  adsorption.

Further analysis revealed that the Pd(II) binding sites within cage 1 form strong bonds with  $\text{SO}_2$  molecules, promoting their oxidation to sulphate species. The presence of hysteresis during gas adsorption, indicative of structural changes, confirmed the chemisorption of  $\text{SO}_2$  onto the metal centres (Fig. 5a). The adsorption enthalpy ( $\Delta H_{\text{ads}}$ ), calculated using the Clausius-Clapeyron method, was approximately  $-50 \text{ J mol}^{-1}$ , signifying a strong interaction. However, this robust cage- $\text{SO}_2$  interaction presents a challenge to the cyclability of the material. Cage 1 experienced a drastic loss of over 99% of its reported adsorption capacity between the first and second cycles. This rapid decline strongly suggests that the adsorbate immediately occupies the primary binding sites, even at low  $\text{SO}_2$  concentrations.

Following this strong binding of  $\text{SO}_2$  gas within cage 1, a significant process of oxidation occurred. The presence of highly oxidising nitrate ions facilitated anion metathesis reactions, effectively converting the initial nitrate salt,  $[\text{Pd}_6\text{L}_8](\text{NO}_3)_{36}$ , into a sulphate salt,  $[\text{Pd}_6\text{L}_8](\text{SO}_4)_{18}$ . Thus, the overarching chemisorption

mechanism observed in cage 1 can be summarised as a two-step process: (1) the strong direct interaction of  $\text{SO}_2$  molecules directly with the Pd(II) metal centres, and (2) subsequent oxidation to sulphate species, driven by the nitrate counterions (see Fig. 5b).

Subsequent research reported in 2024<sup>11</sup> further investigated the application of this Pd(II)-based cage as a catalyst for the surface-mediated conversion of  $\text{SO}_2$  into less hazardous and more manageable sulphate salts. This later work explored the impact of various counterions ( $\text{PF}_6^-$ ,  $\text{BF}_4^-$ , or  $\text{SO}_4^{2-}$ ) on the binding and subsequent oxidation process, moving beyond the initially studied nitrate ( $\text{NO}_3^-$ ).

Interestingly, while  $\text{NO}_3^-$  proved to be the most effective counterion for promoting catalysis, the palladium MOCs incorporating these new counterions still exhibited a high adsorption capacity for  $\text{SO}_2$ . Crucially, with these alternative counterions, the adsorption process became reversible (physisorption), significantly enhancing the material's cyclability (Fig. 5c). This allowed for up to five effective cycles of  $\text{SO}_2$  capture and release.

Another important contribution of this study was the demonstration of binding selectivity for  $\text{SO}_2$  over  $\text{CO}_2$  during surface capture and transformation. A notable selectivity of 78.3 (molar ratio 10 : 90) was achieved, which highlights the potential of these MOCs in targeted  $\text{SO}_2$  removal in mixed gas streams.

The successive investigation into cage 1 for the capture and posterior oxidation of  $\text{SO}_2$  has unveiled previously undocumented characteristics for MOCs interacting with this chemical species (see Table 1). These findings emphasize several key properties that position these MOCs as potential catalysts for  $\text{SO}_2$  transformation, even within complex gas mixtures. The MOCs demonstrated efficient capture and conversion of  $\text{SO}_2$ , with the rate being dependent on the specific counterions incorporated.

The aptitude of these MOCs as effective catalysts for  $\text{SO}_2$  transformation, endorsed by the considerable improvement in the MOCs' ability to be recycled, their resistance to degradation, which is crucial for long-term applications, their selectivity for adsorbing  $\text{SO}_2$  in gas mixtures and simple synthesis methods in water, paves the way for exciting future research.

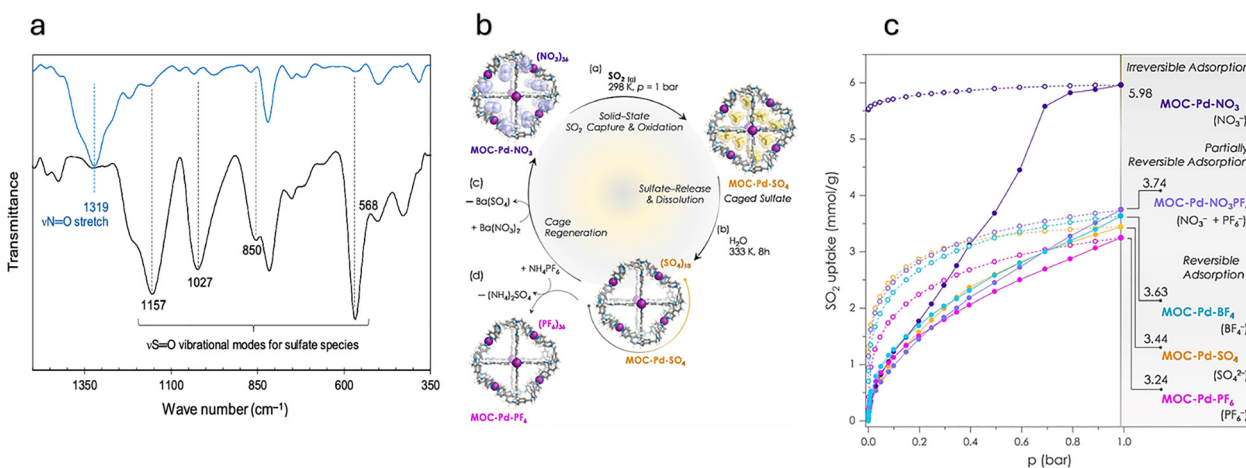


Fig. 5 (a) Change in FTIR spectra before (blue) and after (black)  $\text{SO}_2$  exposure<sup>28</sup> and (b) catalytic cycle of the Pd- $\text{NO}_3$  MOC (cage 1). (c)  $\text{SO}_2$  adsorption-desorption isotherms for palladium-based MOCs with different counterions.<sup>11</sup>



Exploring and analysing MOCs will undoubtedly continue to reveal their fascinating nature and diverse potential applications in environmental remediation and catalysis.

### SO<sub>2</sub>-POCs

As previously discussed, discrete crystalline porous materials offer distinct advantages over extended systems, with their processability in solution being a primary benefit. Porous organic cages (POCs) are constructed through the covalent bonding of organic building blocks, which endows these materials with remarkable chemical and thermal stability.<sup>31,32</sup>

Similar to metal-organic cages, POCs exhibit internal cavities and windows that allow access to guest molecules. They also exhibit solubility in a wide range of common organic solvents. This inherent processability facilitates the development of POC-based interphases, such as thin films or composites, which might not be achievable with other types of porous materials.<sup>32</sup> Consequently, their most conceivable applications lie in gas separation and storage.

Due to their distinctive advantages, POCs have been studied as adsorbents, particularly for gases and pollutants. Among these, the imine known as CC3 stands out. CC3 is a tetrahedral cage synthesized from 1,3,5-triformylbenzene and (R,R)-1,2-cyclohexanediamine. Its derivatives include the reduced secondary amine version (RCC3) and a more rigid tertiary amine functionalization (6FT-RCC3). They are recognised as flexible amine cages with morphological stability under both acidic and basic conditions, and for maintaining porosity in the solid state.<sup>33</sup>

These POCs have demonstrated to retain porosity even after adsorbing gas molecules,<sup>31</sup> and remarkably, even when incorporated into thin films and membranes. Therefore, impressive sorption and permeability capacities have been reported for various gases, such as CO<sub>2</sub>, CH<sub>4</sub>, N<sub>2</sub>, and H<sub>2</sub>, across different exposure interfaces.

However, experimental studies for the corrosive gas SO<sub>2</sub> with POCs had been limited. With research primarily confined to *in silico* modeling of the CC3 cage. Through canonical Monte Carlo simulations, employing the vdW3 force field with double hybrid functional and dispersion correction (B2PLYP-D3), researchers were able to simulate the adsorbate-adsorbent interactions with SO<sub>2</sub> gas molecules.<sup>34</sup> In 2021 the first experimental study specifically focused on SO<sub>2</sub> adsorption by these covalent cages was reported.<sup>12</sup> In that work, CC3, RCC3, and 6FT-RCC3 were selected as SO<sub>2</sub> adsorbents due to the presence of nitrogen in their functional groups, which confers high affinity for interaction with this gas.

The reversibility of the adsorption process was also a key focus, and to complement the experimental findings, computational calculations were performed using density functional theory (DFT) methods, incorporating appropriate approximations, corrections, and parameters. These calculations were performed with Gaussian 16 software and aimed to provide a deeper understanding of the host-guest dynamics. This comprehensive approach allowed for a direct comparison between the experimental results, the computational calculations, and the prior simulations.

Table 1 Comparison of the experimental performance of various stable supramolecular materials for sulfur dioxide (SO<sub>2</sub>) adsorption

| Material                                   | Uptake (0.01–1 bar) at 298 K (mmol g <sup>-1</sup> ) | Surface area (m <sup>2</sup> g <sup>-1</sup> ) | Adsorption type                             | Reversibility   | ΔH° ads (kJ mol <sup>-1</sup> ) | Selectivity (SO <sub>2</sub> : CO <sub>2</sub> ) molar ratio | No. of cycles | Material deterioration           | Ref.      |
|--|--|--|---|---|---------------------------------|--|---------------|----------------------------------|-----------|
| MOF: MIL-101(Cr)-4F(1%)                    | 4.6–18.4   | 2176   | Physisorption [hysteresis at low pressures] | Reversible  | −54.3                           | Not compared   | 50            | Not observed                     | 8         |
| MOF: Mg <sub>2</sub> (dobpdc)              | 3.37–19.5  | 3300   | Physisorption                               | Reversible  | −36.6                           | Greater affinity for SO <sub>2</sub>                         | 50            | Water retention (wet conditions) | 20        |
| COF: SonoCOF-9                             | 0.9–3.5  | 1147   | Physisorption                               | Reversible  | −42.3                           | 12.93 (10:90)  | 50            | Not observed                     | 10        |
| MOC: Pd <sub>6</sub> L <sub>8</sub> Cage 1 | 3.2–6.0  | 111  | Chemisorption/ physisorption                | Irreversible with NO <sub>3</sub> counterions. Reversible with other counterions. | −48.8 to −64.4                  | 25.44 (1:99)<br>78.3 (10:90)                                 | 5             | Not observed                     | 11 and 28 |
| POC: 6FT-RCC3                              | 3.57–13.78   | 396  | Physisorption                               | Reversible  | −43.03                          | Not compared   | 50            | Loss in crystallinity            | 12        |
| HOF: HOF-NKU-1                             | 3.02–6.74  | 200  | Physisorption                               | Reversible  | −50                             | 7331 (10:90)   | 3             | Not observed                     | 40        |

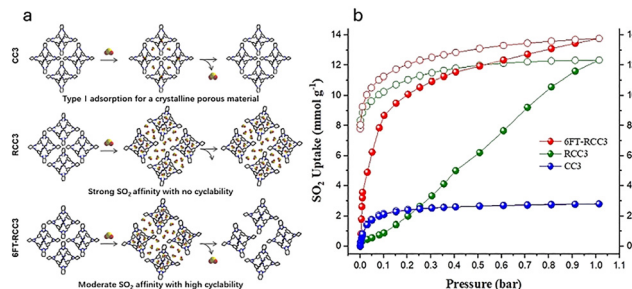


Fig. 6 Three types of amine cages CC3, RCC3, and 6FT-RCC3 (a) interaction with  $\text{SO}_2$  and (b) their corresponding adsorption–desorption isotherms at 298 K and 1 bar.<sup>12</sup>

The experimental results from the three discrete crystalline molecules—CC3, RCC3, and 6FT-RCC3—tested for  $\text{SO}_2$  adsorption revealed varying degrees of capture capacity and reversibility. At 1 bar and 298 K, the amine CC3 demonstrated a modest and reversible  $\text{SO}_2$  capture of 2.78 mmol g<sup>-1</sup>. This figure closely aligned with the previously calculated adsorption capacity of 3.6 mmol g<sup>-1</sup> determined by the B2PLYP-D3 method.<sup>34</sup> In contrast, the secondary amine cage RCC3 achieved a higher capture of 12.34 mmol g<sup>-1</sup>. However, this process proved to be irreversible, characterised by open-loop hysteresis (Fig. 6).

The most promising results were observed with the tertiary amine cage, 6FT-RCC3. This POC achieved the highest amount of adsorbed  $\text{SO}_2$  at 13.78 mmol g<sup>-1</sup> and exhibited excellent reversibility for 50 adsorption–desorption cycles. Despite its relatively small surface area of 396 m<sup>2</sup> g<sup>-1</sup>, this material demonstrated impressive capture capability, coupled with high sensitivity to trace amounts of  $\text{SO}_2$  at low partial pressures (0.1 bar). 6FT-RCC3 is positioning as a strong competitor to higher surface area materials, such as some MOFs,<sup>16</sup> for practical  $\text{SO}_2$  capture applications.

Both 6FT-RCC3 and RCC3 exhibited a moderate degree of similar hysteresis, suggesting a chemisorption process. This chemisorption is driven by a strong bond formed between the R<sub>2</sub>N-H amino functional group on the cages and the  $\text{SO}_2$  molecules.<sup>35</sup> The key difference, however, lies in their regeneration capacities. Vacuum reactivation of 6FT-RCC3 at 80 °C completely restores its original  $\text{SO}_2$  adsorption capacity, which boosts its recyclability.

Another phenomenon shared by both RCC3 and 6FT-RCC3 after  $\text{SO}_2$  exposure is a significant loss of crystallinity. This is attributed to the inherent flexibility of the material combined with the strength of the newly formed N– $\text{SO}_2$  bond.<sup>12</sup> To further understand these interactions, theoretical DFT calculations were performed to determine the host–guest binding energies between the POCs and  $\text{SO}_2$ . A clear trend of increasing experimental adsorption heats was observed from CC3 (49.7 kJ mol<sup>-1</sup>) to 6FT-RCC3 (68.6 kJ mol<sup>-1</sup>) and RCC3: 86.4 kJ mol<sup>-1</sup>. This demonstrates that the amine groups provide strong binding sites for  $\text{SO}_2$  molecules.

The loss of structural crystallinity in porous organic cages is not necessarily a drawback. In fact, amorphous POCs can become even more porous than their crystalline counterparts, being able to reach 898 m<sup>2</sup> g<sup>-1</sup> (Fig. 7).<sup>32</sup> This increased

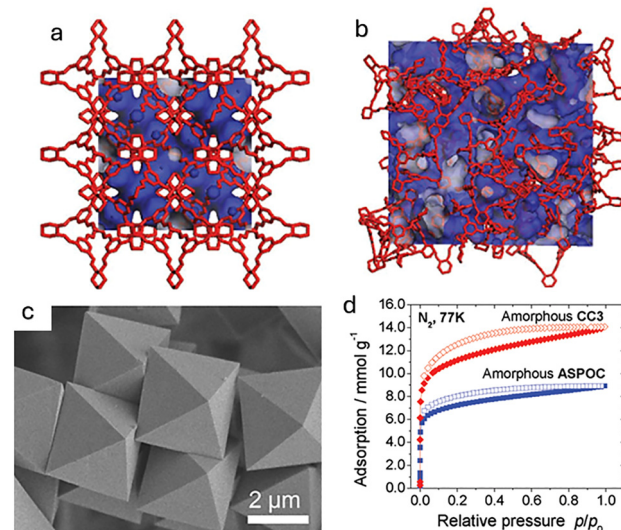


Fig. 7 Structural simulation of (a) crystalline and (b) amorphous CC3 packing, with N<sub>2</sub> molecules (blue) adsorbed. (c) SEM image of CC3 crystals. (d) N<sub>2</sub> adsorption–desorption isotherm of CC3 cage (red) and other amorphous POC, ASPOC (blue).<sup>32</sup>

porosity, combined with their high affinity for  $\text{SO}_2$ , allows the guest molecules to optimize their packing within the porous structure of 6FT-RCC3. A crucial feature of these discrete covalent materials is that, unlike metal–organic frameworks and covalent–organic frameworks, POCs do not lose porosity even when they become amorphous.<sup>33</sup> This unique characteristic, coupled with their excellent processability, synthetic scalability, recyclability, and high sensitivity to  $\text{SO}_2$ , positions POCs with N-rich functional groups, such as 6FT-RCC3, as promising adsorbents for both  $\text{SO}_2$  capture and sensing.

The distinct adsorption behaviors and affinities observed among different POCs make them suitable for a wide array of applications. These discrete covalent materials exemplify the vast potential of supramolecular chemistry and highlight the numerous unexplored opportunities this field offers for developing novel compounds and devices directly applicable to solving real-world problems (Table 2).

## SO<sub>2</sub>-HOFs

The hydrogen bonding interactions that form hydrogen-bonded organic frameworks (HOFs) are weaker than typical coordination or covalent bonds. While HOFs can be constructed from a wide variety of light-element molecules, diaminotriazine (DAT) and carboxylic acid ( $-\text{COOH}$ ) remain the most reported building blocks.<sup>36</sup> The network structure is primarily formed by the N–H bonds and O–H···O interactions from these functional groups. The assembly of small organic molecules through these directional hydrogen bonds results in highly crystalline 2D and 3D supramolecular networks. Even more importantly, this bonding provides a high degree of flexibility to the porous framework, allowing it to deform and regenerate through simple steps.

To maintain their properties and find practical applications, research has focused on standardizing the design of HOFs to



Table 2 Timeline showing milestones in supramolecular chemistry-based materials for the  $\text{SO}_2$  adsorption study in recent years

| UNAM-1<br>First hydrogen-bonded<br>material demonstrates<br>reversible $\text{SO}_2$<br>adsorption<br>2019<br>COF-DC-8 | MOF-177<br>Initial attempt<br>to adsorb $\text{SO}_2$<br>without MOF<br>deterioration<br>2020<br>HOF CB6 | Mg-gallate<br>Selectivity record<br>(325) in $\text{SO}_2/\text{CO}_2$<br>desulfurization<br>processes by MOFs.<br>2021<br>MOC Cage 1 | CC3 Family<br>First $\text{SO}_2$<br>adsorption<br>by POCs'<br>experimental<br>study.<br>2022<br>Mg2(dobpdc) | PI-COF-m10<br>First attempt for<br>cyclic adsorption<br>record by MOFs<br>by COFs, with<br>loss of<br>crystallinity<br>2023 | SJTU-220<br>First $\text{SO}_2$ uptake capacity<br>cyclic adsorption<br>record by MOFs<br>by COFs, with<br>(29.6 $\text{mmol g}^{-1}$ )<br>2024<br>MOC Cage 1 | SonoCOF-9<br>Extremely sensitive<br>COFs withstand<br>cyclical use without<br>deterioration<br>2025<br>HOF-NKU-1 |
|--|--|---|--|---|---|--|
| (2014) CC3 Family <i>In silico</i> simulation of $\text{SO}_2$ mixtures<br>interaction with POCs                       | Reusable HOF parti-<br>cles for separating<br>$\text{SO}_2$ from binary gas<br>mixtures                  | First study exploring<br>the interaction of<br>$\text{SO}_2$ with MOCs  | Successful $\text{SO}_2$<br>separation from<br>gas mixtures<br>using MOFs                                    |   |   | Ultra-selective (7331)<br>$\text{SO}_2$ separation from<br>gas mixtures by<br>HOFs                               |

preserve both their shape and crystallinity. Solvated crystals typically crystallize slowly, forming HOFs. They are also highly sensitive to changes in synthesis parameters like precursor concentration, reaction time, or temperature. However, several studies have proposed decreasing the crystallization rate or increasing the thermal energy as potential solutions for obtaining a more thermodynamically stable phase.<sup>36</sup>

The reversibility of the bonds in HOFs facilitates the regeneration of the system after surface saturation. Recrystallization restores the original porosity and crystallinity of the material.<sup>37</sup> While HOFs have been widely used for gas separation and adsorption, specifically for hydrocarbons, the capture and separation of toxic gases like  $\text{SO}_2$  remains a comparatively under-researched topic. Pioneering work in this field aims to address this gap by studying and reporting significant advancements in using HOFs as an adsorbent and cyclical material for  $\text{SO}_2$  capture.

In 2019, UNAM-1<sup>38</sup> was introduced, which became the cornerstone of this experimental research. UNAM-1 incorporates metal complexes ( $[\text{Cu}^{\text{II}}\text{Cu}_{12}^{\text{I}}(\text{HL})_{12}]^{10-}$ ) as structural elements, which form a perfect octahedral arrangement with  $[\text{Me}_2\text{NH}_2]^+$  (DMAH) cations that interact *via* hydrogen bonds. Most notably, it was the first hydrogen-bonded material to demonstrate reversible  $\text{SO}_2$  adsorption. The material, when activated under mild conditions, achieved a uptake of  $3.5 \text{ mmol g}^{-1}$  at 1 bar. The calculated heat of adsorption for  $\text{SO}_2$  was  $-17.52 \text{ kJ mol}^{-1}$ . This weak interaction results in complete desorption without hysteresis. This work enriched design strategies for multifunctional HOF materials and paved the way for the development of new HOFs specifically designed for this application.

A year later, it was reported that cucurbit[6]uril (CB6)<sup>39</sup> could be used to separate  $\text{SO}_2$  from  $\text{CO}_2$ . CB6 is formed from formaldehyde and glycoluril under acidic conditions. Its main characteristic is a hydrophobic cavity with two symmetrical hydrophilic windows of a smaller diameter. This structure makes it easier for polar molecules like  $\text{SO}_2$  to access the pores, especially with short diffusion paths, *i.e.*, using small particles is better for maximum accessibility.

Nanometric CB6 particles were reported to achieve a capture of  $4.98 \text{ mmol g}^{-1}$  at 1 bar after the first exposure to dry  $\text{SO}_2$ . They exhibited a selectivity of 120 for  $\text{SO}_2$  in mixtures with  $\text{CO}_2$  (10 : 90 molar ratio), which was explained by the difference in

adsorption enthalpy for both gases: a calculated  $-48 \text{ kJ mol}^{-1}$  for  $\text{SO}_2$  and  $-35 \text{ kJ mol}^{-1}$  for  $\text{CO}_2$ . The particles also proved to be highly reusable, maintaining their selectivity and capture capacity for up to 10 adsorption cycles. This reusability makes CB6 a promising material for efficiently separating  $\text{SO}_2$  from binary gas mixtures.

In recent years, advancements in HOFs have focused on improving chemical stability even under harsh conditions. For example, HOF-NKU-1,<sup>40</sup> a material presented in 2025, was activated using a supercritical method, which resulted in a unique and valuable property: dynamic tautomerism. This HOF-NKU-1 interconverts between different structural forms in response to external stimuli; the material can remain deformed after a stimulus and then revert to its original shape. This property is unprecedented for traditional rigid or flexible frameworks.

In the case of HOF-NKU-1, the stimulus is the exposure to  $\text{SO}_2$  itself. As with previous examples, the calculated adsorption enthalpy indicates a much higher-energy interaction ( $>10 \text{ kJ mol}^{-1}$  difference) with  $\text{SO}_2$  molecules than with other gases. The strong interactions result in the deformation of the structure, causing it to display a dominant preference for capturing  $\text{SO}_2$  over any other gas ( $\text{N}_2$ ,  $\text{CO}_2$ , and  $\text{O}_2$ ). A selectivity of 7331 was reported for binary  $\text{SO}_2/\text{CO}_2$  (10 : 90 molar ratio), one of the highest for porous adsorbents. In addition to reaching  $6.74 \text{ mmol g}^{-1}$  of  $\text{SO}_2$  capture at 1 bar. Most impressive is that using a mixture of  $\text{SO}_2/\text{CO}_2/\text{O}_2/\text{N}_2$  (0.3/15/3.5/81.2, v/v/v/v) with 3000 ppm of  $\text{SO}_2$  at a flow rate of  $20 \text{ ml min}^{-1}$ , selective  $\text{SO}_2$  capture was achieved, and its desorption could even be programmed. These advances will mark a turning point in gas separation and storage.

### Contrast with other material classes

Surface modification is one of the most widely used techniques for achieving significant and selective capture.<sup>41</sup> In the case of activated carbon, modifying the surface with amine groups has been shown to promote the chemisorption of  $\text{SO}_2$  in a directly proportional way to the amount of nitrogen added. Activated carbon derived from cellulose-rich sources and doped with  $\text{NH}_3$  groups exhibits the highest saturation capacity, at  $6.25 \text{ mmol g}^{-1}$ .<sup>42,43</sup> This material is also processable; for instance, membranes made from fibers of the same activated carbon type have been reported to continuously remove about



65% of the SO<sub>2</sub> from a SO<sub>2</sub>/CO<sub>2</sub> gas mixture at 3000 ppm over long periods.<sup>44</sup>

In the context of zeolites, modifying them with metal oxides has been used to improve their chemical activity for contaminant removal. Titanium dioxide (TiO<sub>2</sub>), which is widely studied as a photoactive material, has been incorporated into zeolites as a surface dopant to facilitate the removal of SO<sub>2</sub> from contaminated environments. The combination of the photoactive nature of TiO<sub>2</sub> and the adsorptive capacity of zeolites makes heating the zeolites unnecessary to achieve removal, unlike typical methods.<sup>45</sup> The highest SO<sub>2</sub> capture capacity recorded for zeolites is 1.75 mmol g<sup>-1</sup>, which was achieved by K-NaX and F700-0.8-6. Zeolites can remove around 78% of SO<sub>2</sub> from gas mixtures (20% SO<sub>2</sub>, 40% CO<sub>2</sub>, and 40% CO), through dual surface interactions. Based on Lewis base donor-acceptor interactions and hydrogen bonding, these allow for both physisorption and chemisorption, depending on the exposure conditions.<sup>46</sup>

While porous materials like activated carbon and zeolites have long been the industry standard due to their high thermal stability, well-defined pores, and low production costs, recent research highlights their limitations. They tend to be sensitive to moisture, which can reduce both their adsorption capacity and stability. This makes them difficult to use in realistic, humid flue gas flows.<sup>44,46</sup>

In contrast, supramolecular materials can be custom-designed by selecting different organic links and metallic nodes, allowing for the fine-tuning of both pore size and chemical function. This key property enables the pore structures—which are typically fixed in other materials—to be tailored specifically for SO<sub>2</sub> capture.

This design flexibility allows for the creation of materials with exceptionally high selectivity. For example, Mg-gallate,<sup>47</sup> which holds the record for SO<sub>2</sub>/CO<sub>2</sub> selectivity (325), was designed with a large number of hydrogen bond donors lining its pore channels. Additionally, this approach provides a tailored affinity for these molecules. The design of ECUT-11<sup>48</sup> features two distinct cavity apertures (5.4 and 10.2 Å), which allow it to selectively surpass the SO<sub>2</sub> capture capacity of the most commonly reported adsorbents.

Ultimately, while zeolites and other porous materials are currently the leading commercially viable and effective materials for many applications, supramolecular materials represent the next generation of porous adsorbents. Their ability to be designed at the molecular level enables superior performance in terms of selectivity, capture capacity, and reusability even under challenging conditions.

## Conclusions

This perspective synthesises recent and salient experimental contributions in the use of supramolecular chemistry-based materials towards SO<sub>2</sub> capture and detection. Each material exhibits distinct characteristics, which in turn lead to powerful and unique interactions with the guest molecule. The diverse nature of these interactions enriches this field of research,

highlighting how each supramolecular material holds promise for tailored applications, all centered on the interaction with SO<sub>2</sub>.

These materials share key properties like recyclability and porosity, which means their application potential is primarily determined by their specific sensitivity or high capture capacity. Their versatility is highly valued, from use in highly effective sensors that work at low or trace pressures, to gas capture and storage, and their most promising application: the separation of gas mixtures, all while maintaining robust chemical stability. In this ongoing research, discrete materials often offer superior processability, allowing for integration into various interfaces. This opens the door to the design and development of new devices, which is especially useful for flowing gases.

The combined advancements in enhanced stability, record-breaking capture capacities, and improved *in situ* chemical activity are collectively opening a vast new horizon for research. These promising avenues extend beyond merely refining the next generation of materials to include innovative technologies for their design and improvement.

In the near future, the synergy between emerging technologies will result in a vast list of prospective research directions for this application. For example, machine learning could be applied to guide pore engineering or to devise strategies for combining the best qualities into composite materials by new synthesis routes. Furthermore, supramolecular chemistry will be leveraged to create new techniques and devices for a deeper understanding of the adsorption mechanisms of SO<sub>2</sub> and other substances. This field holds immense potential for future growth.

## Author contributions

All authors contributed to writing the original draft, reviewing and editing the manuscript.

## Conflicts of interest

There are no conflicts to declare.

## Data availability

No primary research results, software or code have been included and no new data were generated or analysed as part of this review.

## Acknowledgements

This work was supported by PAPIIT-UNAM (Grant IIN201123), Mexico. A. H. M. acknowledges SECIHTI for the MSc fellowship (1336791). V. M. T. acknowledges the financial support from SECIHTI-Mexico through the program “Convocatoria Ciencia Básica y de Frontera 2023–2024,” grant number CBF2023-2024-2725. P. M. R., thank SECIHTI for the PhD fellowship (1277642).

## Notes and references

- 1 Z. Meng, Y. Liu and D. Wu, *Inhalation Toxicol.*, 2005, **17**, 303–307.



## Highlight

2 K. T. Kuwata, E. J. Guinn, M. R. Hermes and A. B. Fernandez, *J. Phys. Chem. A*, 2015, **119**, 10316–10335.

3 A. L. Reno, E. G. Brooks and B. T. Ameredes, *Environ. Health Insights*, 2015, **9S1**, EHI.S15671.

4 World Health Organization, WHO guidelines for indoor air quality: selected pollutants. WHO Regional Office for Europe, Copenhagen, 2010.

5 M. Matooane and R. Diab, *Arch. Environ. Health*, 2003, **58**, 763–770.

6 Z. Meng, Y. Liu and D. Wu, *Inhalation Toxicol.*, 2005, **17**, 303–307.

7 J. Saravia, G. I. Lee, S. Lomnicki, B. Dellinger and S. A. Cormier, *J. Biochem. Mol. Toxicol.*, 2013, **27**, 56–68.

8 E. Martínez-Ahumada, M. L. Díaz-Ramírez, H. A. Lara-García, D. R. Williams, V. Martis, V. Jancik, E. Lima and I. A. Ibarra, *J. Mater. Chem. A*, 2020, **8**, 11515.

9 K. Biradha, A. Ramanan and J. J. Vittal, *Cryst. Growth Des.*, 2009, **9**, 2969–2970.

10 W. Zhao, J. L. Obeso and V. B. López-Cervantes, *Angew. Chem. Int. Ed.*, 2025, **64**, 1–7.

11 E. G. Percástegui, E. Sánchez-González, S. de J. Valencia-Loza, S. Cruz-Nava, V. Jancik and D. Martínez-Otero, *Angew. Chem. Int. Ed.*, 2024, e202421169.

12 E. Martínez-Ahumada, D. He, V. Berryman, A. López-Olvera, M. Hernandez, V. Jancik, V. Martis, M. A. Vera, E. Lima, D. J. Parker, A. I. Cooper, I. A. Ibarra and M. Liu, *Angew. Chem. Int. Ed.*, 2021, **60**, 17556–17563.

13 F. Huang and E. V. Anslyn, *Chem. Rev.*, 2015, **115**(15), 6999–7000.

14 A. Lund, G. V. Manohara, A. Y. Song, K. M. Jablonka, C. P. Ireland, L. A. Cheah, B. Smit, S. Garcia and J. A. Reimer, *Chem. Mater.*, 2022, **34**, 3893–3901.

15 K. Tan, P. Canepa, Q. Gong, J. Liu, D. H. Johnson, A. Dyevoich, P. K. Thallapally, T. Thonhauser, J. Li and Y. J. Chabal, *Chem. Mater.*, 2013, **25**, 4653–4662.

16 N. K. Gupta, A. López-Olvera, E. González-Zamora, E. Martínez-Ahumada and I. A. Ibarra, *ChemPlusChem*, 2022, **87**(e202200006), 1–9.

17 P. Brandt, A. Nuhnen, M. Lange, J. Möllmer, O. Weingart and C. Janiak, *ACS Appl. Mater. Interfaces*, 2019, **11**, 17350–17358.

18 N. Tannert, Y. Sun, E. Hastürk, S. Nießing, C. Janiak and Z. Anorg, *Allg. Chem.*, 2021, **647**, 1124–1130.

19 J. Li, G. L. Smith, Y. Chen, Y. Ma, M. Kippax-Jones, M. Fan, W. Lu, M. D. Frogley, G. Cinque, S. J. Day, S. P. Thompson, Y. Cheng, L. L. Daemen, A. J. Ramirez-Cuesta, M. Schröder and S. Yang, *Angew. Chem., Int. Ed.*, 2022, **61**, e202207259.

20 E. Martínez-Ahumada, D. Kim, M. Wahiduzzaman, P. Carmona-Monroy, A. López-Olvera, D. R. Williams, V. Martis, H. A. Lara-García, S. López-Morales, D. Solis-Ibarra, G. Maurin, I. A. Ibarra and C. S. Hong, *J. Mater. Chem. A*, 2022, **10**, 18636.

21 W. Gong, Y. Xie, A. Yamano, S. Ito, X. Tang, E. W. Reinheimer, C. D. Malliakas, J. Dong, Y. Cui and O. K. Farha, *J. Am. Chem. Soc.*, 2023, **145**(49), 26890–26899.

22 W. Gong, P. Gao, Y. Gao, Y. Xie, J. Zhang, X. Tang, K. Wang, X. Wang, X. Han, Z. Chen, J. Dong and Y. Cui, *J. Am. Chem. Soc.*, 2024, **146**(46), 31807–31815.

23 S. Ge, K. Wei, W. Peng, R. Huang and E. Akinlabi, *Chem. Soc. Rev.*, 2024, **53**, 11259.

24 G.-Y. Lee, J. Lee, H. T. Vo, S. Kim, H. Lee and T. Park, *Sci. Rep.*, 2017, 7.

25 Z. Meng, R. M. Stoltz and K. A. Mirica, *J. Am. Chem. Soc.*, 2019, **141**, 11929–11937.

26 J. Wang, J. Wang, W. Zhuang, X. Shi and X. Du, *J. Chem.*, 2018, 1–8.

27 M. T. Lv, M. D. Cui, K. P. Bai, Y. Jiang, W. P. Chen, N. N. Sun, X. Q. Hu, C. Huang, Q. Y. Yang and Y. Z. Zheng, *Angew. Chem. Int. Ed.*, 2025, e202506838, 1–9.

28 S. de J. Valencia-Loza, A. López-Olvera, E. Martínez-Ahumada, D. Martínez-Otero, I. A. Ibarra, V. Jancik and E. G. Percástegui, *ACS Appl. Mater. Interfaces*, 2021, **13**, 18658–18665.

29 Z. Yang, G. Liu, Y. D. Yuan, S. B. Peh, Y. Ying, W. Fan, X. Yu, H. Yang, Z. Wu and D. Zhao, *J. Membr. Sci.*, 2021, **636**, 119564.

30 Z. Y. Zeng, Z. C. Lou, L. Hu, W. Dou, X. Zhao, X. Li, J. Fang, X. Qian, H. B. Yang and L. Xu, *Chem. Eng. J.*, 2024, **496**, 154091.

31 T. Tozawa, J. T. Jones, S. I. Swamy, S. Jiang, D. J. Adams, S. Shakespeare, R. Clowes, D. Bradshaw, T. Hasell, S. Y. Chong, C. Tang, S. Thompson, J. Parker, A. Trewin, J. Bacsá, A. M. Slawin, A. Steiner and A. I. Cooper, *Nat. Mater.*, 2009, **8**, 973–978.

32 Q. Song, S. Jiang, T. Hasell, M. Liu, S. Sun, A. K. Cheetham, E. Sivaniah and A. I. Cooper, *Adv. Mater.*, 2016, **28**, 2629–2637.

33 M. Liu, M. A. Little, K. E. Jelfs, J. T. A. Jones, M. Schmidtmann, S. Y. Chong, T. Hasell and A. I. Cooper, *J. Am. Chem. Soc.*, 2014, **136**, 7583–7586.

34 W. Li and J. Zhang, *J. Comput. Chem.*, 2014, **35**, 174–180.

35 Z. Xu, Y. Ye, Y. Liu, H. Liu and S. Jiang, *Chem. Commun.*, 2024, **60**, 2261–2282.

36 L. Chen, B. Zhang, L. Chen, H. Liu, Y. Hua and S. Qiao, *Mater. Adv.*, 2022, **3**, 3680.

37 B. Han, H. Wang, C. Wang, H. Wu, W. Zhou, B. Chen and J. Jiang, *J. Am. Chem. Soc.*, 2019, **141**, 8737–8740.

38 R. Dominguez-Gonzalez, I. Rojas-Leon, E. Martínez Ahumada, D. Martínez-Otero, H. A. Lara-García, J. Balmaseda-Era, I. A. Ibarra, E. G. Percastegui and V. Jancik, *J. Mater. Chem. A*, 2019, **7**, 26812–26817.

39 J. Liang, S. Xing, P. Brandt, A. Nuhnen, C. Schlüsener, Y. Sun and C. Janiak, *J. Mater. Chem. A*, 2020, **8**, 19799–19804.

40 L. Li, X. Zhang, X. Lian, L. Zhang, Z. Zhang, X. Liu, T. He, B. Li, B. Chen and X. H. Bu, *Nat. Chem.*, 2025, **17**, 727–733.

41 A. A. Abdulrasheed, A. A. Jalil, S. Triwahyono, M. A. A. Zaini, Y. Gambo and M. Ibrahim, *Renewable Sustainable Energy Rev.*, 2018, **94**, 1067–1085.

42 J. P. Boudou, *Carbon*, 2003, **41**, 1955–1963.

43 J. P. Boudou, M. Chehimi, E. Broniek, T. Siemieniewska and J. Bimer, *Carbon*, 2003, **41**, 1999–2007.

44 V. Gaur, R. Asthana and N. Verma, *Carbon*, 2006, **44**, 46–60.

45 J. Yu, J. Kiwi, T. Wang, C. Pulgarin and S. Rtimi, *J. Photochem. Photobiol. A*, 2019, **375**, 270–279.

46 D. Tefera-Zewdie, Y. Desta-Bizualem and A. Gashu-Nurie, *Discover Appl. Sci.*, 2024, **6**, 331.

47 F. Chen, D. Lai, L. Guo, J. Wang, P. Zhang, K. Wu, Z. Zhang, Q. Yang, Y. Yang, B. Chen, Q. Ren and Z. Bao, *J. Am. Chem. Soc.*, 2021, **143**, 9040–9047.

48 M. J. Yin, X. H. Xiong, X. F. Feng, W. Y. Xu, R. Krishna and F. Luo, *Inorg. Chem.*, 2021, **60**, 3447–3451.

